

Ionic space-charge effects in polymer light-emitting diodes

J. C. deMello, N. Tessler, S. C. Graham, and R. H. Friend
Cavendish Laboratory, Madingley Road, Cambridge, CB3 0HE, United Kingdom
(Received 19 November 1997)

We report measurements and modeling studies of organic light-emitting diodes (LED's) with mobile ions incorporated into the active polymer layer, similar in structure to the light-emitting electrochemical cells (LEC's) reported by Pei *et al.* We show that movement of the ions, rather than electrons or holes, is responsible for the Ohmic electrode-polymer contacts observed in these devices. We show that for typical devices with polymer film thicknesses of 1000–2000 Å, concentrations of ions greater than 10^{20} cm⁻³ are required for efficient electroluminescent behavior. We show also that under steady-state operation, the electric field is very low in the bulk of the polymer, and that the electron and hole currents are therefore driven mainly by diffusion. Quantitative modeling of electron-hole recombination matches observed emission profiles.
[S0163-1829(98)10219-9]

I. INTRODUCTION

Semiconducting conjugated polymers are promising materials for the development of inexpensive thin-film electroluminescent displays.^{1,2} Much work in recent years has concentrated on improving device characteristics such as efficiencies, drive voltages lifetimes, and peak brightnesses. The basic LED comprises a luminescent polymer sandwiched between two electrodes, of which at least one must be transparent.¹ The electrical properties of such a device are strongly dependent on the nature of the contacts between the polymer and the electrodes, and also on the mobilities of electronic carriers within the polymer film. In order to maximize the electroluminescence (EL) efficiency of an organic LED, it is important to balance the rate at which electrons and holes are injected into the polymer bulk.² Hence, for diodes that comprise a single polymer layer, the barriers to electron and hole injection must be of a similar height and thickness. The exact sizes of the barriers depend on factors such as the work functions of the electrodes, interfacial states, and the existence of interfacial layers between the electrodes and the polymer. Interfacial properties can be modified by use of different electrodes; however, this is often at the expense of electrode stability.^{3–6}

A means of improving the injection characteristics of electroluminescent devices was reported by Pei *et al.*⁷ They fabricated devices similar in structure to a conventional LED, but with mobile ions incorporated into the polymer layer. Ions are relatively immobile in most conjugated polymers, but when blended with a polymer electrolyte, a composite film is formed in which both ionic and electronic carriers are mobile.^{8,9} Poly(ethylene-oxide) (PEO) is a well-studied polymer electrolyte¹⁰ in which lithium triflate readily dissolves to form predominantly free ions.¹¹ The devices fabricated by Pei *et al.* comprised a solid-state blend of poly(*p*-phenylene-vinylene) (PPV) and PEO, to which a quantity of lithium triflate had been added. The ratio of PPV: PEO: lithium triflate was 1:1:0.2 by weight, corresponding to an ionic density of about 1 mole dm⁻³ (10^{21} cm⁻³). The polymer layer was sandwiched between indium tin oxide (ITO) and aluminium electrodes. Pei *et al.*

reported significant improvements in the EL efficiencies of these devices compared with conventional diodes and attributed this to an improved balance in the injection rates for electrons and holes. They suggested that an electrochemical doping process¹² resulted in the formation of oxidized and reduced chains of PPV that were electrically compensated by nearby counter ions. Because both oxidized and reduced PPV are good electronic conductors, it was argued that the interfaces should behave Ohmically. The position at which the oxidized and reduced layers meet in the bulk of the device was considered to be the region of recombination and light emission. On the basis of the proposed mechanism, Pei *et al.* referred to these devices as light-emitting electrochemical cells (LEC's). However, the notion of doping requires some discussion. There is little evidence for any binding between individual ions and associated electronic charges, and predictions based on an analogy with chemical doping may be misleading. In this paper, we propose an electrodynamic model for device operation. We explain how the accumulation of ionic space charge in the vicinity of the electrodes gives rise to large electric fields that reduce the widths of the barriers to electronic carrier injection. In this model, the reduction in effectiveness of the interfacial barriers is due to the displacement of ions, and does not require the presence of an electrically conducting or "doped" polymer. The probabilities for hole and electron injection are greatly enhanced relative to a conventional LED and as a result high EL efficiencies are observed.

We present in Sec. II a range of experiments that we have carried out to extend the work of Pei *et al.* Specifically, we have studied the transient response of the current through the devices on application of a steady voltage, the dependence of the electrical characteristics on ionic concentration, and the variation of emitted light with applied bias. Results from these experiments are used to characterise the different roles of mobile ions and electronic charges in these devices; the results are found to be well described by the model developed in Sec. III. We provide a brief overview of the model here. The conjugated polymer and ionic transport matrix form a blend in which both ionic and electronic charge carriers are mobile. Under an applied external field, anions drift

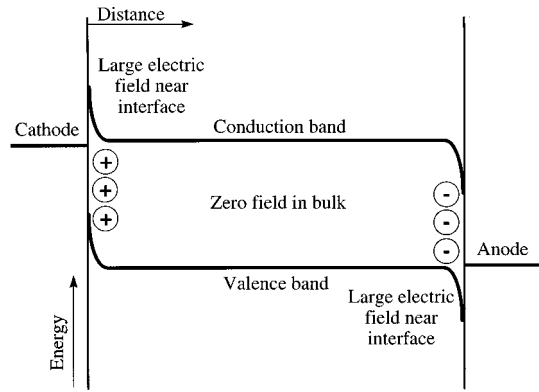


FIG. 1. A schematic band diagram for an LEC device operating in forward bias. Positive ionic space charge accumulates close to the cathode. Negative ionic space charge accumulates close to the anode. This redistributes the electric field away from the bulk of the device towards the interfaces. The steady-state shape of the barriers for electron and hole injection are set by solutions to Poisson's equation and Boltzmann statistics. Typically the barrier widths are less than 10 \AA in a device of thickness 1000 \AA with an ionic charge density in excess of 10^{20} cm^{-3} .

to the positive electrode and cations to the negative electrode until drift and diffusion currents are equalized. Because the density of ionic charge in a typical device is very high ($>10^{20} \text{ cm}^{-3}$), small movements of these ions can give rise to very large electric fields.

Under conditions of constant applied bias, ionic charge redistribution occurs throughout the bulk of the polymer film until the local electric field has been cancelled everywhere. A finite electric field can only be sustained at the interfaces, where the motion of the ions is blocked by the electrodes. This gives the band diagram shown schematically in Fig. 1. The diagram shows the situation at the onset of electronic carrier injection (for equal barriers to electron and hole injection). Notice that, as drawn, the barrier widths for electron and hole injection are very small; in a device of width 1000 \AA and with an ionic concentration of 10^{20} cm^{-3} , we calculate them to be less than 10 \AA in thickness. Any difference between the barrier heights will lead to a mismatch in the rate at which electrons and holes are injected and will therefore limit the EL efficiency. This mismatch decreases as the barrier widths are reduced and the transmission coefficients tend to unity. If the barriers are made sufficiently thin, the impedances of the interfaces become so low that they can be neglected, and large fluxes of electronic charges can be injected from the electrodes. Further rearrangement of the ions then occurs, until the magnitude of the electric field in the bulk of the device is again zero. Under these conditions, a steady-state electronic current can be sustained in which electronic charges are transported solely under the influence of diffusion. This steady-state but nonequilibrium situation (an external bias is required) has some of the characteristics of a "doped" conducting polymer: electronic space charge in an electrochemically doped polymer is compensated by ionic charge so as to achieve overall charge neutrality.

We summarize here the main conclusions of our work. The ionic concentration controls the nature of the device characteristics. For example, we will show that for a typical device of thickness 1000 \AA , significant improvements in de-

vice performance are achieved only when the ionic concentration is greater than 10^{20} cm^{-3} (Secs. II D, III C 1, and III C 2). At concentrations in excess of 10^{20} cm^{-3} and under conditions of constant applied bias, the electric field is negligible in the bulk of the device, but is very large close to the contact interfaces. Symmetric current-voltage characteristics (Sec. III E) are expected only at high concentrations. At concentrations smaller than about 10^{19} cm^{-3} , the electric field extends through the full thickness of the device, and rectification is expected for devices that use metals with differing work functions as electrodes (Sec. III C 2). In the high-concentration case, unipolar carrier injection is expected at biases below the band gap of the polymer (defined as the free-energy difference between positive and negative polarons in the polymer film), switching to bipolar injection at applied biases greater than the band gap (Secs. III D and III F 2).

II. EXPERIMENTAL RESULTS

In this section, we provide a range of measurements that illustrate the effects of ions on the electrical characteristics of polymer light-emitting devices. We also report measurements of light emission as a function of applied bias and demonstrate that light emission is detectable at biases significantly lower than the band gap of the conjugated polymer.

A. Device fabrication

Devices were fabricated from a blend of PPV and PEO of molecular mass 10^5 , and lithium triflate. Films were spin cast onto glass substrates coated with ITO from a 20:5: x (by weight) mixture of the standard sulfonium precursor polymer to PPV,¹ PEO, and lithium triflate dissolved in a 6:1 (by volume) mixture of acetonitrile and water. After drying, films were heated at $180 \text{ }^\circ\text{C}$ for 12 h under a vacuum of 10^{-6} mbar. The final films were about 2000 \AA in width. Films were fabricated with four ionic concentrations, estimated to be $\leq 10^{18}$ ($x=0$), 10^{18} ($x=0.01$), 10^{19} ($x=0.1$), and 10^{20} cm^{-3} ($x=1$). A relatively high ratio of PPV to PEO was used in order to minimize the degree of phase separation in the polymer films. Other groups¹³ have used a 1:1 (by weight) blend of PPV and PEO that allows a higher maximum ionic concentration to be supported. The absence of optical scattering by the polymer films indicated phase separation between the polymer components to be on a scale smaller than the wavelength of visible light. Aluminium contacts were evaporated on top of the polymer films under a vacuum of approximately 10^{-5} mbar. The devices were operated at room temperature under a vacuum of 10^{-2} mbar.

B. Transient response of the external current on application of a constant applied bias

Studies were carried out on an LEC device fabricated with an ionic concentration of 10^{20} cm^{-3} . The two electrodes were shorted together for 200 s before a measurement was made in order to ensure that steady state had been reached. A steady voltage V was then applied across the electrodes ($t=0$) with the ITO contact wired as the anode.

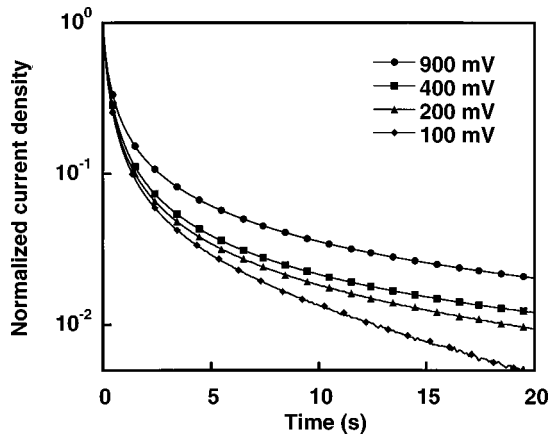


FIG. 2. Normalized data showing the transient response of the current in the external circuit for applied biases in the range $0 < V < 1$ V. Data has been normalized to permit easier comparison of transient responses.

Figures 2 and 3 show the time dependence of the current in the external circuit for applied biases between 100 mV and 2.6 V.

Figure 2 shows data in the range $0 < V < 1$ V. The decay profiles are very similar for all sets of data and the transient lifetime is approximately constant in this range. The transient response of the current is determined by the motion of the ions in response to the applied field (see Sec. III G 1). There is a gradual increase in the steady-state current as the applied bias is raised, corresponding to an increase in the rate of thermally assisted carrier injection.

Figure 3 shows data at higher applied biases. Electronic carrier injection becomes significant at biases in excess of 1.4 V, at which bias the current transient becomes structured. There are several features of the profile that should be noted. Initially, there is a decrease in current similar in form to that seen in Fig. 2 (corresponding to the accumulation of uncompensated ionic space charge at the two electrodes). This decay continues until a minimum is reached, at which point electronic charge (hole) injection begins. The current increases to a maximum value (as the impedances of the con-

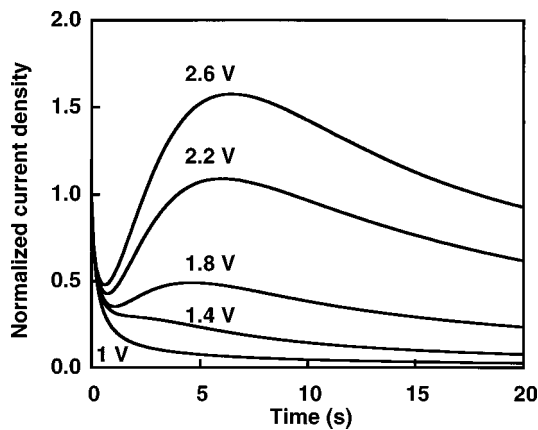


FIG. 3. Normalized data showing the transient response of the current in the external circuit for applied biases in the range $1 < V < 2.6$ V. Injection of holes into the polymer layer occurs at biases in excess of about 1.4 V. Data has been normalized to permit easier comparison of transient responses.

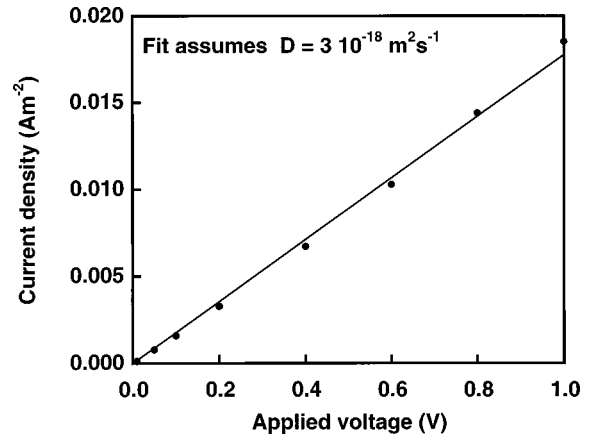


FIG. 4. Data showing the variation of the external current measured at time $t=0$ with applied bias. The straight-line fit is the result of a numerical simulation assuming an effective ionic diffusivity of $3 \times 10^{-18} \text{ m}^2 \text{ s}^{-1}$ and no binding between ions.

tacts fall towards zero), and then decays away slowly towards a steady-state value (at which stage no electric field is present in the bulk and large electric fields exist only near the contacts). The existence of a local maximum is significant. As is discussed in Sec. III G 2, it is due to contributions to the total current from both drift and diffusion components; in contrast, the steady-state current is due to diffusion only.

C. Ohmic behavior of the ionic current

Figure 4 shows the variation of the current at time $t=0$ with applied bias for the sample measured in the previous section. Ionic charge transfer is a slow process and ions accumulate slowly at the electrodes. Electronic carrier injection will not occur until a significant amount of charge has accumulated at the electrodes. When the external field is first applied (and before the ions have moved), the electronic current should be similar to that seen in a device with no ions. The steady-state current-voltage characteristics for a device without ions are shown in Fig. 5 and the electronic current density is seen to be very small (in fact it is less than

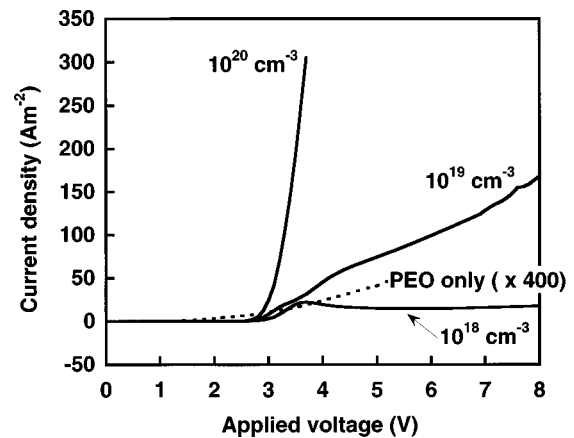


FIG. 5. Data showing steady-state current-voltage characteristics for devices fabricated with differing ionic concentrations operating in forward bias. The curve for the device fabricated without any added lithium triflate has been enlarged by a factor of 400 for clarity.

0.0003 A m⁻² at 1 V). This justifies our association of current with ion motion. The linear response is modeled in terms of ion drift (see Sec. III G 1). The solid line through the data points is a numerical fit assuming no binding between the ions and an effective diffusivity for positive and negative ions of $3 \times 10^{-18} \text{ m}^2 \text{ s}^{-1}$. (This estimated diffusivity is similar in magnitude to values quoted for other polymer electrolytes that typically vary from 10^{-18} to $10^{-14} \text{ m}^2 \text{ s}^{-1}$ at ambient temperature.¹⁴ It is somewhat below the values reported for pure PEO at room temperature ($10^{-16} \text{ m}^2 \text{ s}^{-1}$) because phase separation between the two polymers in the blend hinders ionic transport. Ionic conductivities can be improved significantly by using a surfactant to bind the conjugated polymer to the electrolyte.¹⁵) Figure 2 shows only a slight change in the transient profile as the applied bias is increased. If a sizeable binding energy existed between the ions, we would expect to see a superlinear increase in initial current and an increase in the transient decay rate as the applied bias was increased. Because this behavior is not observed, we conclude that the ions are effectively unbound for the range of concentrations used here. We note that departures from Ohmic behavior are observed when significant binding exists between ions.¹⁶

D. Dependence of the current-voltage characteristics on the concentration of ions in the polymer film

Figure 5 shows the steady-state current-voltage characteristics for devices fabricated with differing ionic concentrations. The devices were prebiased for approximately 15 s before making each measurement, and the applied bias was incremented in steps of 0.1 V. The characteristic decay time for the ionic transient in these devices was no longer than 3 s.

The current-voltage characteristics show a strong dependence on the ionic concentration. The experimental curves for $x=0$ ($\ll 10^{18} \text{ cm}^{-3}$) and $x=0.01$ (10^{18} cm^{-3}) indicate the current flow to be heavily restricted for these devices. However, ionic effects do become noticeable when the concentration is raised to 10^{19} cm^{-3} ; at any given applied bias, the curve for $x=0.1$ (10^{19} cm^{-3}) shows a much larger steady-state current than devices with lower ionic concentrations. For devices with ionic concentration greater than 10^{20} cm^{-3} , charge injection is greatly improved and the current rises very sharply with applied bias. We discuss in Secs. III C 1 and III C 2 the effects of ionic concentration on the electronic injection characteristics.

E. Light-voltage characteristics of LEC devices with high ionic concentrations

Figure 6 shows the variation in luminescence intensity with applied bias for an LEC fabricated with an ionic concentration of 10^{20} cm^{-3} ($x=1$). Light is detectable at biases as low as 2.0 V. Since this is below the optical gap of PPV (2.4 eV) and therefore well below the free-energy difference for electrons and holes, we consider that it arises from radiative recombination of injected holes with thermally excited electrons. We note that 2.0 V represents the detection limit for this experiment, set by the photomultiplier tube sensitivity, and does not represent a real threshold for light emission. It has been suggested by Yu *et al.*¹⁷ that the ‘‘onset’’ in light

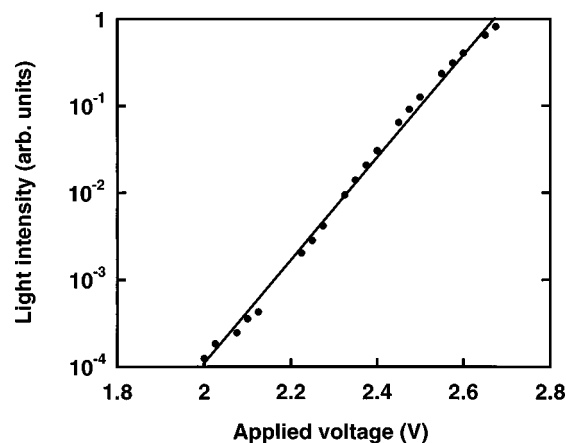


FIG. 6. Data showing the variation in luminescence intensity with applied bias. Note that light is detectable at biases lower than the optical gap of PPV (2.4 eV).

emission occurs at a bias equal to the optical gap of the polymer. This was considered to provide evidence that electroluminescence resulted from the radiative recombination of unbound electron-hole pairs. The data shown in Fig. 6 do not support this model. We observe that our data are similar in form to those presented by Yu *et al.*, but the lowest applied bias at which light is detectable has been reduced to 2.0 V (Yu *et al.* were unable to detect light at biases below 2.4 V), perhaps owing to the use of more sensitive detection equipment. The issue of the electroluminescence threshold is well studied for inorganic semiconductors. For example, the observation of emission at voltages lower than the forbidden energy gap is discussed by Ivey for the case of ZnS.¹⁸ Here too, detector sensitivity was identified as the origin of a perceived threshold.

III. MODEL FOR DEVICE OPERATION

In order to understand the range of measurements presented in Sec. II and many of the results reported in the literature, we have formulated an electrodynamic model. Device behavior follows directly from the Coulombic interaction of the ions, electrons, and holes. Materials capable of supporting motion of both electrons and ions are relatively uncommon, but the thermodynamic properties of such mixed conductors have been studied in detail by Wagner¹⁹ and Weppner.^{20,21}

A. Assumptions of the model

The model is electrodynamic in nature and does not introduce a binding energy between the ions and conjugated polymer. It is assumed that the electrodes are ionically blocking, and that the ions are not discharged at the electrodes. The ions, electrons, and holes interact only through Coulombic forces, and the transport of charge carriers is due to drift and diffusion. The contact interfaces between the electrodes and the polymer are treated as ideal. (Any oxide layers existing at the interfaces are assumed to be sufficiently thin that they pose no additional barrier to electronic transport.) In addition, we assign a single well-defined energy gap to the polymer, although in a real polymer a distribution of conjugation lengths, and hence energy gaps, will exist.

We consider here the case where the ions are free. At high ionic concentrations, however, ion-pair formation is expected when attractive interactions between anion and cation are significant. In other words, an equilibrium exists for the process $MX \rightleftharpoons M^+ + X^-$. By the law of mass action, as the concentration of salt is increased, the concentration of ion pairs increases at the expense of free ions. The effect of ion-pair formation is an overall reduction in the effective density of ionic charge.²² This is undesirable in an LEC for the reasons given in Sec. III C 1. It also greatly complicates an understanding of the ionic conductivity. Ion-pair motion results in a transfer of mass but not of charge. This leads to a departure from Ohmic conductivity and to drag effects on ions.¹⁶ The tendency to form ion pairs depends on the properties of the anion. It is preferable to select an anion X^- that behaves as a weak Lewis base,¹⁶ otherwise the X^- ion will have a tendency to form an ion pair with the complexed M^+ . A simple study of the functional dependence of ionic conductivity on salt concentration, has shown that Li^+ and $CF_3SO_3^-$ are totally dissociated in PEO/polyurethane networks for ionic concentrations as high as 10^{21} cm^{-3} .^{11,16} Therefore, lithium triflate is a good choice of salt in LEC devices. It has been suggested elsewhere²³ that a binding energy of about 0.6 eV might exist between the oppositely charged ions. The experimental results presented in Sec. II C are consistent with a model in which the ions are predominantly dissociated. (If significant phase separation exists between the two polymers, local regions of high ionic charge density may exist giving rise to enhanced binding).

B. Density of intrinsic electronic carriers at biases below the threshold for electronic carrier injection

For a device in open circuit, the average density N of electrons (or holes) in the conduction (or valence) band of a semiconductor can be estimated using Boltzmann statistics. The devices discussed in this paper were fabricated using PPV with ITO and aluminium electrodes, as explained in Sec. II A. In this case, the barrier to hole injection δh is about 0.2 eV (Ref. 24) and the barrier to electron injection δe is about 1.0 eV [as determined for example from measurements of the maximum photovoltage in Al/PPV/ITO LED's (Ref. 25)]. An upper limit for N is provided by a calculation that ignores the effects of ion drift (in which case the electric field is uniform across the entire polymer film). Taking $\delta e = 1 \text{ eV}$ and $\delta h = 0.2 \text{ eV}$, we calculate the average density of electronic carriers in the polymer film to be very much smaller than 10^{15} cm^{-3} . This compares with average ionic densities in excess of 10^{20} cm^{-3} found in a typical LEC. The assumption that the polymer layer contains many more ions than electrons and holes is therefore valid.

C. Roles of the ions, electrons, and holes in determining the characteristics of the electrode-polymer interfaces in LEC devices

We discuss here the roles of the ions and the injected electrons and holes in determining the characteristics of the interfaces. We discuss how the ions account for low interfacial impedances, and how these impedances are further modified by the injected charge carriers.

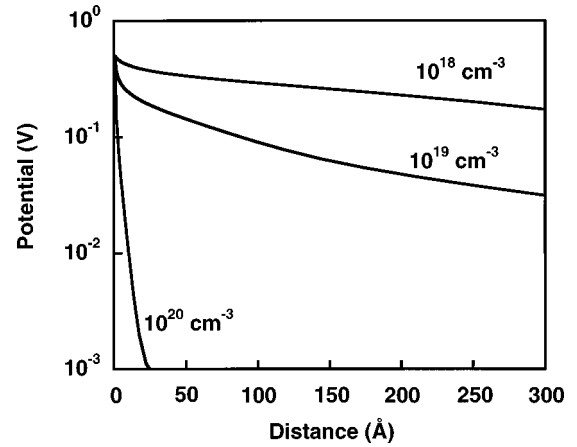


FIG. 7. Numerical simulations for the profiles of the electric potential in the vicinity of one electrode, calculated for devices with different ionic concentrations. The LEC device thickness is 1000 Å.

1. Effects of the ions in determining the distribution of the electric field through the polymer film

The steady-state ionic charge distributions can be determined from Poisson's equation and Boltzmann statistics that together account for drift and diffusion effects. If a voltage is applied between the polymer and the electrode, it is possible to derive an analytical expression for the distribution of the steady-state electrical potential by imposing the boundary conditions that $\Phi = V$ at the electrode and $E = 0$ far from the electrode. This is the approach taken in Debye-Hückel theory^{26,27} and is an acceptable approximation for a thick device ($d \gg 10 \mu\text{m}$).

However, Debye-Hückel theory does not describe well the potential distribution in a thin device. It is difficult to obtain an analytical solution using the real boundary conditions ($\Phi = -V/2$ at one electrode and $\Phi = +V/2$ at the other) and we therefore employed a numerical simulation using drift-diffusion and Poisson equations. This also allowed the time-dependent evolution of the charge distributions and electric field to be observed. The resolution of the simulation was $\pm 5 \text{ Å}$.

Figure 7 shows the profile of the steady-state potential for an applied bias of 1 V determined numerically for a device of thickness 1000 Å. We arbitrarily define the width of the potential barrier at a temperature T (taken to be room temperature in this study) to be the distance over which the potential falls to a value kT/e . At an ionic concentration of 10^{18} cm^{-3} , an almost constant electric field extends through the bulk of the polymer, and the presence of the ions has only a small effect. At a concentration of 10^{19} cm^{-3} , the effect of the ions is stronger, but the electric field still extends more than 300 Å into the polymer bulk. At a concentration of 10^{20} cm^{-3} , the electric field extends about 5 Å into the polymer bulk.

The model does not allow for the finite volume of the ionic charges and when the calculated width of the field is less than the ionic radius, the excess ionic charge will in reality be confined to a monolayer. The ionic charge in the monolayer is compensated by electronic charge on the electrode. A double-layer is formed and from simple electrostatics the potential difference $\Delta\phi$ between the electrode and the polymer bulk is given by

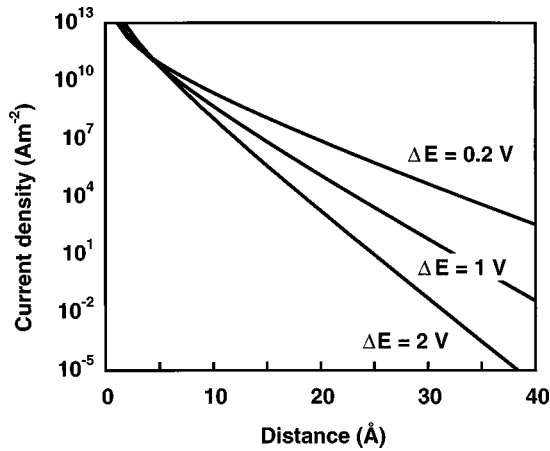


FIG. 8. The tunnelling current through a triangular barrier, calculated according to Fowler-Nordheim theory, Eq. (2). The results for barrier heights of 0.2, 1, and 2 eV are shown.

$$\Delta\Phi = \frac{r_{\text{ion}}\sigma}{\epsilon_0\epsilon_r}, \quad (1)$$

where r_{ion} is the ionic radius and σ is the surface-charge density. In the case of lithium ions, the ionic radius is approximately 0.68 Å and therefore a maximum surface-charge density of about $7 \times 10^{19} \text{ m}^{-2}$ can be attained. A single monolayer can therefore support a maximum possible potential difference of about 90 V if $\epsilon_r = 1$.

2. Charge injection from the electrodes into the polymer film

We model the current across the interfacial barriers using Fowler-Nordheim theory.²⁸ For wide barrier widths, other models (for example the Onsager model) which take into account scattering of the injected carriers by the lattice are more appropriate.²⁹ However, these considerations do not apply when the barrier width is smaller than a characteristic hopping length. We assume that injection of charge carriers occurs into a well-defined energy state.

The current is only weakly sensitive to the shape of the barrier³⁰ and a good estimate of the current density j can be obtained by assuming injection into the conduction band through a triangular barrier for which we can write

$$j = \alpha \frac{\Delta E^2}{x^2} \exp\left[-\frac{8\pi}{3h} (2em^*)^{1/2} (\Delta E)x\right]. \quad (2)$$

Here, e is the electronic charge, m^* is the effective mass of the electron in the polymer (which we take to be equal to the free electron mass), ΔE is the height of the barrier and d is its width. α is a proportionality-constant which is about $10^6 \text{ A m}^2 \text{ V}^{-2}$ for a typical metallic electrode.²⁸

Fowler-Nordheim theory is used to calculate the electronic current-density as a function of barrier-width in Fig. 8. Again, we consider an Al/PPV/ITO device of thickness 1000 Å. The barrier to electron injection is the larger of the two barriers and is approximately 1 eV. From Fig. 8, it is clear that the electron current densities in the devices with ion concentrations of 10^{18} and 10^{19} cm^{-3} will be heavily restricted ($\ll 100 \text{ A m}^{-2}$) and these devices will be inefficient as EL diodes. When the ionic current density is increased to 10^{20} cm^{-3} , the width of the region where an electric field

is present is reduced to about 5 Å. From Fig. 8, the cathodic interface can then support electron current densities in excess of 10^{10} A m^{-2} .

The results of this analysis match the experimental results shown in Fig. 5. Carrier injection is somewhat improved for ionic densities in excess of 10^{19} cm^{-3} , and is hugely enhanced for carrier concentrations in excess of 10^{20} cm^{-3} .

In addition to the current flowing from the metal into the semiconductor, a diffusion current will also flow from the semiconductor to the metal. *Backdiffusion* is a well-known phenomenon in inorganic semiconductor device physics, the net effect of which is to increase the contact resistance.³¹ The backflow current is highest for semiconductors with low electronic mobility. Recently, the importance of backdiffusion in organic semiconductor devices (specifically Al/MEH-PPV/ITO LED's) has been demonstrated by Davids *et al.*³² They show that quasiequilibrium can be assumed to exist across the interfacial barriers, owing to the low mobility of charge carriers in these polymers. That is, the current is limited by the finite mobilities of carriers in the polymer bulk rendering the interfacial impedances negligible. This situation is modified somewhat by the injected electronic charge as we discuss in Sec. III C 3.

3. Modification of the interfacial impedances by the injected electrons and holes

In Secs. III C 1 and III C 2 we discussed how the accumulation of uncompensated ionic space charge at the electrodes modifies the widths of the interfacial barriers permitting easy injection of electronic carriers into the polymer film. The injection of these electronic carriers causes a further modification of the interfacial impedances as we discuss below.

The contacts determine the effective density of carriers supplied by each electrode. An upper limit for the carrier densities at the electrodes is imposed by the density of ionic charge. We have assumed throughout that the density of ionic carriers is far higher than the density of electronic carriers. Under this assumption, the interfacial barriers are very thin and charge can easily be injected from the electrodes into the polymer film. However, the density of electronic charge must necessarily remain lower than the density of ionic charge. The narrowing of the interfacial barriers relies on the existence of uncompensated space charge near the electrodes: positive charge near to the cathode and negative charge near to the anode. When the density of electronic charge approaches the density of ions, these regions of uncompensated space charge are removed; the electric field is therefore redistributed away from the interfacial regions, widening the interfacial barriers and discouraging further injection of electronic charge. This feedback mechanism between the density of injected charge and the interfacial impedances imposes an upper limit on the effective density of carriers supplied by each electrode. We consider this to be limited to no more than a few percent of the average ionic density.

A lower limit on the density of electronic charge in an operational LEC can be obtained using the observation by Dick *et al.* of photoluminescence (PL) quenching in operational planar devices of thickness 10 μm and with ionic density 10^{21} cm^{-3} .³³ PL quenching occurs as a result of exci-

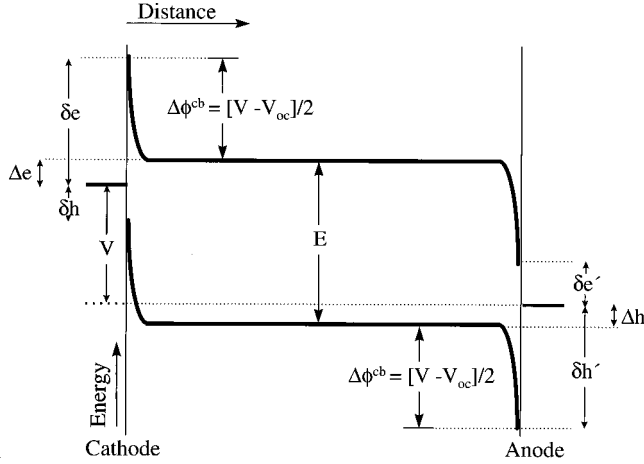


FIG. 9. A schematic band diagram for an LEC with a high density of ionic charge ($>10^{20} \text{ cm}^{-3}$). The applied bias is insufficient for the injection of electronic carriers.

ton migration to a quenching site, which in this case will be a nearby electron or hole. Estimates of the diffusion range of excitons in PPV range from 80 to 130 Å (Refs. 34 and 35) from which we expect quenching effects to become apparent when the density of polarons is greater than 10^{17} cm^{-3} . (It is interesting to note that the ionic charges do not behave as quenching sites for the excitons, even though they are predominantly dissociated in the polymer film.³⁶ Using an integrating sphere measurement,³⁷ we have found the external PL quantum efficiency to be unaffected by the presence of ions. The quantum efficiency for a 1000-Å film containing no ions prepared from a 1:1 (by weight) blend of PEO and poly-[2-methoxy-5-(2'-ethyl)-hexyloxy-*p*-phenylenevinylene] (MEH-PPV) was measured to be 8%. This efficiency was unchanged in films with ionic densities of 10^{21} cm^{-3} .)

From consideration of the PL quenching and the feedback mechanism described above, we estimate that the density of electrons and holes supplied by the contacts is somewhere between 10^{17} and 10^{19} cm^{-3} in the devices fabricated by Dick *et al.* For the devices reported in this paper (which have smaller ionic concentrations of 10^{20} cm^{-3}), the upper limit on the electronic concentration is about 10^{18} cm^{-3} .

D. Calculation of the threshold-biases for the injection of electronic carriers from the electrodes into the bulk of the polymer film

In Sec. III C, we considered tunnelling of electrons and holes through thin interfacial barriers into the bulk of the polymer film. The relative positions of the Fermi levels of the electrodes and the energy levels of the polymer are also important in controlling charge injection into the polymer. We consider here the existence of threshold biases, above which charge injection is possible.

Figure 9 is a schematic representation of a device with an ionic concentration $\geq 10^{20} \text{ cm}^{-3}$ subject to a subthreshold applied bias V . Below the threshold for electronic-carrier injection, the electric field is equal at each electrode. Suppose the barrier to electron injection at the cathode is δe , the barrier to hole injection at the anode is $\delta h'$, and the free-

energy difference between positive and negative charge carriers is E . Other variables are defined in Fig. 9. We note that

$$\delta e + \delta h = E, \quad (3)$$

$$\delta e' + \delta h' = E. \quad (4)$$

The potential difference $\Delta \phi^{\text{ca}}$ between the cathode and the anode is equal to the difference between the applied bias V and the open-circuit voltage, V_{oc} :

$$\Delta \phi^{\text{ca}} = V - V_{\text{oc}}. \quad (5)$$

However,

$$V_{\text{oc}} = \delta e' - \delta e, \quad (6)$$

so that

$$\Delta \phi^{\text{ca}} = V + \delta e - \delta e'. \quad (7)$$

The potential barriers at the two electrodes are symmetric; their shape depends only on the applied bias and the concentration of ionic charge. The difference in potential between the cathode and the bulk of the polymer film $\Delta \phi^{\text{cb}}$ is therefore one half of $\Delta \phi^{\text{ca}}$:

$$\Delta \phi^{\text{cb}} = \frac{1}{2} \Delta \phi^{\text{ca}} = \frac{1}{2} [V + \delta e - \delta e']. \quad (8)$$

Hence, the difference in potential Δe between the Fermi level of the cathode and the edge of the conduction band in the bulk of the polymer film is

$$\Delta e = \delta e - \Delta \phi^{\text{cb}}, \quad (9)$$

$$\Delta e = \frac{1}{2} [\delta e + \delta e' - V]. \quad (10)$$

Using Eq. (4), we can then write

$$\Delta e = \frac{1}{2} [E + \delta e - \delta h' - V], \quad (11)$$

$$\Delta h = \frac{1}{2} [E - \delta e + \delta h' - V]. \quad (12)$$

The injection of electronic charge without thermal assistance is possible only when one of these expressions becomes negative:

$$V_{\text{threshold}} = E + \delta e - \delta h' = \delta e + \delta e' \quad (13)$$

(threshold for electron injection if $\delta e < \delta h'$),

$$V_{\text{threshold}} = E - \delta e + \delta h' = \delta h + \delta h' \quad (14)$$

(threshold for hole injection if $\delta e > \delta h'$).

If the barrier heights to electron and hole injection are of equal magnitude, injection of both carrier types will occur at a bias equal to E . If, however, $\delta e \neq \delta h'$, then the injection of electrons and holes will begin at different biases. Suppose the barrier to hole injection is smaller. In this case, hole injection will begin at a bias, somewhat lower than E , given by Eq. (14). The polymer will therefore acquire a net positive charge which discourages further injection of holes. The Fermi level of the anode is therefore effectively pinned to the valence band of the polymer until electron injection begins. In order to satisfy the boundary conditions, a greater fraction of the internal field must be dropped near the cathode than the anode. The threshold for injection of the second carrier

type should coincide with the band gap of the polymer E . Double injection is only observed at biases in excess of E . We will consider the unipolar and bipolar regimes in greater detail in Secs. III F 1 and III F 2.

For the Al/PPV/ITO devices fabricated in the present study appropriate values are $\delta e = 1$ eV, $\delta h' = 0.2$ eV, and $E = 2.4$ eV. Hence, we expect hole injection to occur first at a bias equal to 1.6 V. Electron injection will follow at a bias above 2.4 V. Experimentally, the hole current becomes comparable to the ionic current at an applied bias of 1.4 V (Fig. 3). This is slightly lower than the injection threshold for holes derived above; we attribute this to the distribution of energy gaps in the polymer, thermally assisted hole injection, and uncertainty in the barrier heights at the electrodes.

E. Symmetry in the current-voltage characteristics in forward and reverse bias

A characteristic feature reported for many LEC devices is an absence of rectification.³⁸ This follows naturally in our model, from the observation that Eqs. (13) and (14) are symmetric in primed and unprimed variables. Since these variables are characteristics of the cathode and anode materials, respectively, interchanging the electrodes does not alter the device thresholds.

F. Device operation in steady state

We calculate here the distributions of electrons and holes in the polymer film under conditions of constant applied bias. Device operation is considered in both the unipolar regime and the bipolar regime.

1. Unipolar injection regime

In Sec. III D, we discussed the existence of a unipolar charge injection regime at applied biases in the range $V_{\text{threshold}} < V < E$. We will assume that $\delta h' < \delta e$ and that the average density of ionic carriers greatly exceeds the average density of electrons and holes. In the unipolar regime, the polymer acquires a positive charge and therefore its potential is raised relative to the anode. Positive charge will accumulate in the polymer until the Fermi level of the anode and the valence band of the polymer are aligned. Because charge neutrality is maintained in the bulk, the excess charge must be stored at each interface. We can therefore roughly model the device as two parallel plate capacitors, each with a plate spacing of several angstroms. Owing to the pinning of the Fermi level of the anode to the valence band of the polymer, the potential difference across the anodic interface is equal to $\delta h'$ and the potential difference across the cathodic interface is equal to $V + \delta e - E$. If the steady-state hole current through the device is also known, it is possible to determine the average density of holes in the device.

We consider a device in a steady state for which the electric field will be sizeable only at the interfaces (Sec. III C 1). Owing to the absence of an electric field in the bulk of the device, the injected holes will move under the influence of diffusion only. From Fick's law we therefore expect a linear drop in hole concentration across the device from a value of n_h^0 near the anode to a value of zero at the cathode. Note that the ions redistribute themselves in order to maintain charge

neutrality in the bulk. The steady-state current j_h is related to n_h^0 , the diffusivity of the holes D_h , and the device thickness d by

$$j_h = -\frac{D_h n_h^0}{d}. \quad (15)$$

Here, we have ignored the effects of the interfaces that typically account for less than one percent of the total device thickness.

2. Bipolar injection regime i (local neutrality holds)

At biases in excess of the band gap E , injection of both electrons and holes is possible. Charge transport still occurs under the influence of diffusion only, but there now exists the possibility of electron-hole recombination. Ignoring the thicknesses of the interfacial regions, the steady-state electronic charge distributions n_h and n_e are governed by the coupled second-order differential equations:

$$D_e \nabla_x^2 n_e = k_{eh} n_e n_h - k_{eh} n_i^2, \quad (16)$$

$$D_h \nabla_x^2 n_h = k_{eh} n_e n_h - k_{eh} n_i^2, \quad (17)$$

where D_e and D_h refer to the diffusivities of the charge carriers, n_i refers to the thermal generation of electron-hole pairs, and k_{eh} is the rate constant for electron-hole recombination. This is different from the form used by Riess and Cahen^{39,40} who have recently reported a model for the bipolar injection regime. They assume $k_{eh} n_e n_h = k_{eh} n_i^2$, which is only true when current-induced recombination is negligible in comparison with thermal recombination. This is certainly not the case in an operational LEC, since the light output is far higher than the thermal (blackbody) radiation for an object at the temperature of the device. n_e can be eliminated from Eqs. (16) and (17) to yield the single second-order differential equation:

$$\nabla_x^2 n_h = \frac{k_{eh}}{D_e} n_h^2 - \frac{k_{eh} n_h^0}{D_e} n_h + \frac{k_{eh} n_h}{D_e D_h} [D_h n_h^0 + D_e n_e^d] \frac{x}{d} - \frac{k_{eh}}{D_h} n_i^2, \quad (18)$$

where d is the device width and we have also used the boundary conditions, $n_h|_{x=d} = n_e|_{x=0} = 0$, $n_h|_{x=0} = n_h^0$, and $n_e|_{x=d} = n_e^d$.

In order to simplify the equation, we define $a = n_e^d/n_h^0$ and $b = D_e/D_h$. We also make the change of variables $u_h = n_h/n_h^0$, $u_e = n_e/n_e^d$, and $y = (1+ab)(x/d) - 1$. Equation (18) then reduces to Eq. (19):

$$\nabla_y^2 u_h = \frac{k_{eh} d^2 n_h^0}{D_h b (1+ab)^2} \left[u_h (u_h + y) - b \frac{n_i^2}{(n_h^0)^2} \right] \quad (-1 < y < ab). \quad (19)$$

Similarly,

$$\nabla_y^2 u_e = \frac{k_{eh} d^2 n_h^0}{D_h b (1+ab)^2} \left[u_e (abu_e - y) - b \frac{n_i^2}{(n_h^0)^2} \right] \quad (-1 < y < ab). \quad (20)$$

We estimate a density of thermally generated charge carriers of order 10^7 m^{-3} in PPV at room temperature. This is clearly very much smaller than the carrier densities at the electrodes, and we therefore neglect the second term in the square brackets.

The ratio k_{eh}/D_h can be estimated using Langevin theory,⁴¹

$$\frac{k_{eh}}{D_h(1+b)} = \frac{e^2}{kT\epsilon_r\epsilon_0}. \quad (21)$$

Hence Eqs. (19) and (20) can be rewritten:

$$\nabla_y^2 u_h = \left[\frac{(ed)^2 n_h^0}{kT\epsilon_r\epsilon_0} \right] \frac{1+b}{b(1+ab)^2} u_h(u_h + y) = k_0 u_h(u_h + y), \quad (22)$$

$$\begin{aligned} \nabla_y^2 u_e &= \left[\frac{(ed)^2 n_h^0}{kT\epsilon_r\epsilon_0} \right] \frac{1+b}{b(1+ab)^2} u_e(abu_e - y) \\ &= k_0 u_e(abu_e - y), \end{aligned} \quad (23)$$

where k_0 is defined implicitly. The physical meaning of the quantity k_0 is complicated; it is related to the probability of electron-hole capture, which we will show is effectively unity for values of k_0 greater than about 100. This means that the external EL efficiencies in LEC devices with large k_0 are limited not by the capture probability, but rather by nonradiative decay channels such as polaronic quenching of excitons. [It is interesting to note that Eqs. (22) and (23), and consequently the steady-state charge distributions, are independent of the absolute diffusivities of the electrons and holes; only the relative diffusivities of the charge carriers are important. This is a consequence of using the Langevin relation between diffusivities and the capture rate for electrons and holes.]

Equations (22) and (23) are nonlinear, and we were unable to find an analytical solution. We solved the equation numerically using a deferred correction technique and Newton iteration. The profile of the emitted light can be determined from the product of n_h and n_e . Note that y is a reduced spatial coordinate, selected so that the recombination zone is always centered at $y=0$. The location x_0 of the center of the recombination zone in real spatial coordinates follows from the definition of y and is given by

$$x_0 = \frac{d}{1+ab}. \quad (24)$$

x_0 is sensitive to both the relative mobilities of carriers in the polymer and the relative density of carriers supplied by the electrodes. For example, an increase in either the density of carriers supplied by the cathode or the diffusion coefficient of the electrons would move the recombination zone closer to the anode.

A typical device of width 1000 \AA is considered in Fig. 10. We have assumed $a=1$, $b=0.25$, and $n_h^0=10^{18} \text{ cm}^{-3}$ (see

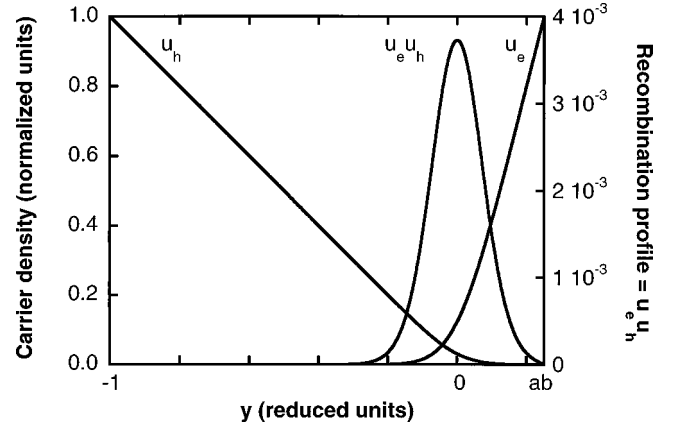


FIG. 10. Electronic charge distributions in a device of width 1000 \AA that is operating in the bipolar charge injection regime; we have assumed $a=1$, $b=0.25$, and $n_h^0=10^{18} \text{ cm}^{-3}$. The distributions are calculated from numerical solutions to Eqs. (22) and (23). The spatial profile of the recombination rate (as calculated from the product $u_e u_h$) is also shown. The x axis is expressed in the reduced coordinates of y for which $-1 < y < ab$. For $k_0 > 100$, the normalized recombination profile is usually Gaussian in shape to a very good approximation. Deviations from Gaussian behavior are expected only if the recombination zone is situated very close to one of the electrodes ($\Delta y \approx ab$); this will occur if there is a large mismatch between either the electron and hole mobilities or the density of carriers at the two supplying electrodes.

Sec. III C 3, which are reasonable values and help to illustrate some of the general properties of solutions to Eqs. (22) and (23); k_0 is equal to 5800 for these values. The spatial profiles of the carrier densities u_e and u_h are shown in Fig. 10. The product $u_e u_h$, which describes the profile of the recombination zone, is also shown.

For values of k_0 greater than about 100, the shape of the recombination profile, $u_e u_h$, is well described by a Gaussian function, Eq. (25); the least-squares correlation coefficient is typically better than 0.9995. Equations (25)–(27) provide a convenient empirical means of calculating the solutions to Eqs. (22) and (23) without the need to repeat the numerical analysis described above. These equations may be used directly when extracting physical parameters from experimental data:

$$u_e u_h = \xi \exp\left\{ \frac{-y^2}{2\sigma^2} \right\}. \quad (25)$$

σ and ξ are found to obey the empirical relations defined by Eqs. (26) and (27), respectively. The area underneath the profile of $u_e u_h$ is $1/abk_0$.

$$\sigma = 1.36 \left(\frac{1}{k_0^{1/3}} \right), \quad (26)$$

$$\xi = 0.30 \left(\frac{1}{abk_0^{2/3}} \right), \quad (27)$$

$$\sigma \xi = \frac{1}{\sqrt{2\pi}} \left(\frac{1}{abk_0} \right). \quad (28)$$

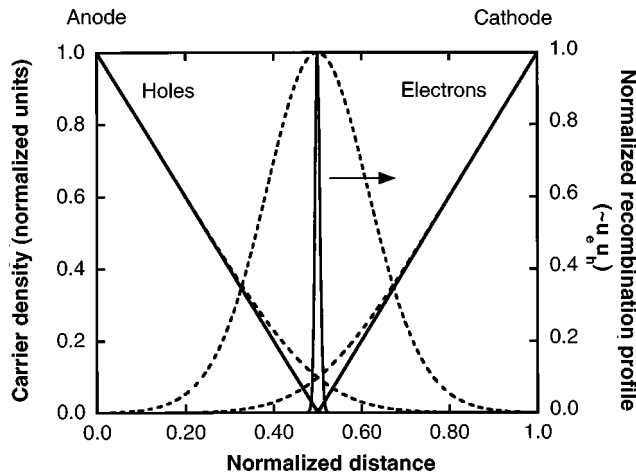


FIG. 11. Comparison of the spatial profiles of u_e , u_h , and $u_e u_h$ for devices of width 1000 Å (dotted lines) and 10 μm (solid lines). The calculation assumes carrier densities of 10^{18} cm^{-3} at the two supplying electrodes and equal mobilities for electrons and holes. The width of the recombination zone as a fraction of the total device width is very much smaller for the thicker device. The x axis is normalized to the thickness of the device.

Using the definition of y , we can relate the width of the recombination zone as a fraction of the real device thickness to σ by

$$\frac{\Delta x}{d} = \frac{\Delta y}{(1+ab)} = \frac{2\sigma}{(1+ab)}. \quad (29)$$

(We note that deviations from Gaussian behavior arise if the recombination zone is situated too close to one of the electrodes ($\sigma \approx ab$); this will occur if k_0 is small (less than 100) or if there is a large mismatch between either the electron and hole mobilities or the density of carriers at the two supplying electrodes. Equations (25), (26), and (27) are inappropriate in such cases, and it is necessary to numerically solve Eqs. (22) and (23) for the specific values of a , b , and k_0 . Leakage currents are expected at the electrodes, and therefore the EL efficiency will be limited by the probability of electron-hole capture.)

Assuming $k_0 > 100$ and $\sigma \ll ab$, the steady-state current through the device can be determined from Eq. (30), which follows directly from the forms of the charge distributions shown in Fig. 10:

$$j = \frac{-D_h n_h^0 (1+ab)}{d}. \quad (30)$$

For $k_0 > 100$ and $\sigma \ll ab$, $\nabla_y u_e|_{y=-1} = 0$ and $\nabla_y u_h|_{y=ab} = 0$, so there are no leakage fluxes of electrons and holes at the counter electrodes. In other words, all injected carriers recombine before they reach the opposite electrode. Therefore the probability of electron-hole capture is unity, as mentioned earlier.

From Eqs. (26) and (29), $\Delta x/d \propto 1/k_0^{1/3} \propto 1/d^{2/3}$, and therefore the width of the recombination zone as a fraction of the total width of the polymer film decreases slowly with increasing values of d (for fixed values of a , b , and n_h^0). For example, in Fig. 11 we show the results for devices of thickness 1000 Å and 10 μm . We have assumed carrier densities

of 10^{18} cm^{-3} at the two supplying electrodes, and equal mobilities for electrons and holes. Under these assumptions, recombination occurs in the center of the device. Emission occurs throughout the bulk of the 1000-Å film. In the 10- μm device the recombination zone is reduced to a thin strip in the center. Experimental measurements on planar LEC devices have verified this to be the case.³³ This emission zone has been interpreted by Pei *et al.* as the intersection of chemically n - and p -doped polymer forming an “*in situ pn junction*.” Implicit in the description of the pn junction under forward bias is the presence of a high electric field in this recombination zone. We stress that in our model, the electric field is zero in the recombination zone.

We mention here the results of an optical beam induced current (OBIC) measurement by Dick *et al.* that have been used as evidence for the existence of a pn junction.³³ In this experiment, a planar device of width 20 μm and approximate ionic concentration 10^{21} cm^{-3} was used. A fixed bias was applied to the device at room temperature until steady state had been achieved. The device was then cooled down to a temperature of 250 K, at which temperature the ions are essentially immobile. Having frozen in the ionic distribution, the applied bias was removed. A focused excitation source was scanned across the device and the maximum photovoltage was measured as a function of the position of the excitation. The spatial resolution was limited by a beamwidth of approximately 1 μm . The measured photovoltage was largest in the approximate centre of the device corresponding to the existence of a large electric field there.⁴² Dick *et al.* argued that this confirmed the existence of a pn junction in the center of the device. However, direct comparisons between a device treated in this way and an operational device may be misleading. In the process of cooling the device there is a change in the distribution of electronic carriers (because the relative mobility of electrons and holes changes with temperature). Further ionic redistribution is therefore required to bring the device into steady state again. However, owing to the falling ionic mobility, this process of ionic redistribution becomes slower as the temperature falls. If the sample is cooled too rapidly it is possible to *freeze in* a metastable distribution of charge carriers in which the ions do not compensate completely for the electrons and holes. The situation is further complicated by the removal of the applied bias, following which action electrons and holes in the vicinity of the recombination zone are able to recombine. The observed electric field in the bulk of the device is caused by the uncompensated ionic charge resulting from these two effects. Limitations in resolution imposed by the wide beam-width prevent the very thin electric fields at the two interfaces from registering in the measurement.

3. Bipolar injection regime ii (local neutrality does not hold)

At high applied biases, the assumption of charge neutrality in the bulk may break down, in which case charge transport will occur under the influence of both drift and diffusion. This regime has been discussed both by Smith²³ and by Riess and Cahen,^{39,40} although the two treatments are based on different assumptions. We do not attempt a detailed analysis here, but make a few general comments concerning device operation under conditions of high carrier injection. As the applied bias is raised above the band gap of the poly-

mer, we expect the barriers to charge injection to increase in width. If this were not the case, a huge flux of injected carriers would pass through the device, a phenomenon that is not observed experimentally; the current density passing through the device with an ionic concentration of 10^{20}cm^{-3} in Fig. 5 is approximately 300 A m^{-2} at an applied bias of 3.5 V. For biases just in excess of the band gap, a field-free region is still expected in the bulk of the device. As the applied bias is raised further, a steady increase in the barrier widths and a consequent reduction in the width of the field-free region will occur. At sufficiently high biases, the field-free region will no longer exist. An electric field will now be present through the entire thickness of the device. The actual bias at which the assumption of a field-free bulk breaks down is sensitive to several parameters: the concentration of the ions, the magnitude of the binding energy between positive and negative ions, the electrode materials, and the mobility of electrons and holes in the polymer.

G. Transient response of devices

In this section we consider the transient response of the external current when a steady voltage is applied to the device. We examine again the response measured experimentally in Sec. II B, and show that it is consistent with the model proposed here.

1. Transient behavior in ion-only regime

So far, we have only considered the steady-state behavior of the devices. Consider a device that has been in short circuit for a long period of time. When a voltage V is applied across the electrodes, ionic charges flow until drift and diffusion currents match. Equilibrium is then reached and the net ionic current throughout the device is zero. In the regime where very few electronic carriers are present in the polymer film, we can relate the electronic current in the external circuit to the motion of ions using Maxwell's fourth equation:

$$j_{\text{ext}}(t) = j_{\text{ion}}^p(x,t) + j_{\text{ion}}^n(x,t) + \epsilon_0 \epsilon_r \frac{\partial E(x,t)}{\partial t}, \quad (31)$$

where $j_{\text{ext}}(t)$ refers to the measured current density in the external circuit, $j_{\text{ion}}^p(x,t)$ refers to the positive ions, $j_{\text{ion}}^n(x,t)$ refers to the negative ions, and $E(x,t)$ refers to the electric field in the device. The temporal variation in the ionic fluxes and the electric field can be determined numerically from drift and diffusion equations if the mobilities of the ions are known. Equation (31) then gives the transient in the external circuit.

2. Transient behavior in unipolar regime

The form of the transient response shown in Fig. 3 is consistent with the model presented here. The transient current in the range $V_{\text{threshold}} < V < E$ is determined by the interplay of the ions, the injected holes, the interfacial impedances and the electric field in the bulk of the device. All of these contributions to the external current are coupled together. For convenience we divide the transient response at drive voltages above $V_{\text{threshold}}$ into the four regimes described below.

Suppose a bias in excess of $V_{\text{threshold}}$ is applied to a device. The ions can only react slowly to the applied external field owing to their relatively low mobilities. Initially, the resultant internal electric field is equal to the sum of the applied external field and the original internal field. The field through the bulk of the device is therefore initially uniform to a good approximation.

Regime 1: (times less than 1 s, as shown in Fig. 3). As the ions drift towards the appropriate electrodes, the internal field is moved away from the bulk of the polymer towards the interfaces. The current in the external circuit is governed entirely by this ionic redistribution and decreases in accordance with Eq. (31).

Regime 2: (times between about 1 and 7 s, as shown in Fig. 3) The ionic redistribution causes a narrowing of the barriers to electronic injection. This progressively reduces the interfacial impedances and a hole current develops. As this occurs and the interfacial impedances are reduced, a gradual increase in the hole current occurs. (At 2.6 V we also expect a contribution from an electron current.)

Regime 3: (times between about 7 and 20 s as shown in Fig. 3). Because there is a nonzero electric field in the bulk of the device, holes move under the influence of both drift and diffusion in this regime. The continuing redistribution of ionic charge caused by the presence of the electric field in the bulk of the polymer reduces the magnitude of this field and therefore reduces the drift contribution to the electronic current. Numerical studies confirm that this process of reducing the bulk electric field continues long after the interfacial barriers have become negligibly thin. A smooth decay in the external current is therefore observed as the electric field decays away to zero.

Regime 4: (times beyond about 20 s). Eventually steady state is reached. In this regime, the final ionic distribution ensures that the electric field in the bulk of the device is zero. No drift current is present and all charge transport occurs under the influence of diffusion. The external current is entirely due to the flux of holes passing through the device and is governed by Eq. (15) (Sec. III F 1).

We consider the data shown in Fig. 3 provides direct evidence for the model proposed here. It is difficult to rationalize the complex behavior of the transient current at the voltages shown in Fig. 3 in terms of alternative models.

IV. A COMPARISON OF LED'S AND LEC'S

We have proposed a mechanism in which the accumulation of ionic charge at the electrodes causes a redistribution of the internal electric field. If the density of ionic charge is sufficiently high ($>10^{20}\text{ cm}^{-3}$), then the electric field is negligible in the bulk of the device and very large at the interfaces. In Fig. 12, we compare a conventional LED and an LEC, just before the onset of electronic charge injection. In this range, the density of electronic carriers is approximately governed by Boltzmann statistics and is very much smaller than 10^{15} cm^{-3} (Sec. III B). The LED therefore behaves like a parallel plate capacitor with a constant electric field extending throughout the device. In the LEC the internal electric field is divided equally between two narrow regions, one positioned at the cathode and the other at the anode. Everywhere else in the device the electric field is

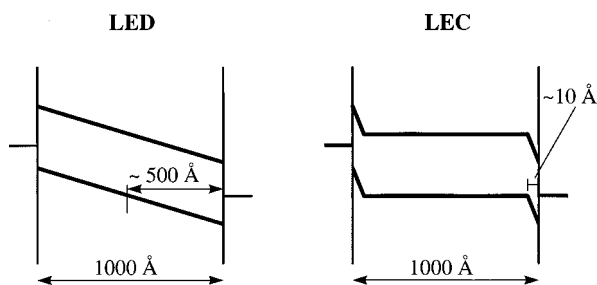


FIG. 12. Schematic band diagrams showing an LED and an LEC ($>10^{20} \text{ cm}^{-3}$) weakly biased in the forward direction. The LED resembles a capacitor with plate spacing of 1000 Å. The LEC resembles two capacitors in series each having a typical plate spacing of less than 10 Å.

negligible. Clearly the barrier widths are very much smaller in the LEC than in the LED. In an LEC, charge injection occurs as soon as sites lower in potential than the Fermi level of one of the electrodes become available. In an LED, however, the barriers are too thick for charge injection to occur when suitable sites first become available. Only at significantly higher biases are the barriers thin enough for significant charge injection to occur. Hence typical operating voltages for LED's are much higher than those for LEC's.

V. CONCLUSIONS

We have presented a model that can explain the major features of LEC behavior. The presence of ionic charge redistributes the internal electric field towards the electrodes. The profile of the internal electric field is very sensitive to the ionic concentration. In order for the presence of ions to have a significant effect, the ionic density must be in excess of 10^{20} cm^{-3} . At significantly lower ionic concentrations, a linear electric field extends through the whole device as in a

conventional LED. When the density of ionic charge is higher than 10^{20} cm^{-3} , the barriers are only a few angstroms in width and provide low impedance to the passage of charge. The interfaces, therefore, behave Ohmically and the choice of the electrode materials does not greatly affect device performance. A "turn on" in the current is predicted at biases somewhat lower than the optical band gap and symmetric current-voltage characteristics are anticipated. Unlike LED's, EL efficiency in thick LEC's is believed to be limited mainly by the electron-hole capture probability and the (PL) quantum yield of the luminescent polymer.

Devices have been fabricated with varying densities of ionic charge. The behavior of these devices is consistent with the model summarized above. The time dependence of the current gives useful insight into the injection mechanism. The transient characteristics are consistent with the existence of free ions in the polymer film (however, binding may occur between ions at concentrations in excess of 10^{20} cm^{-3}). Although the presence of PEO inhibits electron transport, the steady-state electronic characteristics improve significantly as the ionic concentration is raised. The efficiency of the devices fabricated with an ionic density of 10^{20} cm^{-3} was about 0.2% (external quantum efficiency in the forward direction). In LED's fabricated with the same electrodes, the measured efficiency was two orders of magnitude lower. This is consistent with an improvement in the balance of injection rates for electrons and holes in an LEC compared with an ordinary LED. Light emission is visible at biases below the optical gap of the conjugated polymer. Perceived thresholds in light emission correspond to limitations in detector sensitivity.

ACKNOWLEDGMENTS

We thank J. Owen and P. Bartlett for valuable discussions and J. J. M. Halls for his considerable help with this work.

- ¹J. H. Burroughes *et al.*, *Nature (London)* **347**, 539 (1990).
- ²N. C. Greenham and R. H. Friend, in *Solid State Physics*, edited by H. Ehrenreich and F. A. Spaepen (Academic, New York, 1995), Vol. 49, p. 2.
- ³P. Dannetun *et al.*, *Synth. Met.* **67**, 133 (1994).
- ⁴P. Dannetun *et al.*, *J. Chem. Phys.* **100**, 6765 (1994).
- ⁵P. Dannetun *et al.*, *Mol. Cryst. Liq. Cryst.* **230**, 43 (1993).
- ⁶P. Dannetun *et al.*, *J. Chem. Phys.* **99**, 664 (1993).
- ⁷Q. B. Pei *et al.*, *Science* **269**, 1086 (1995).
- ⁸C. M. Berthier and R. H. Friend, U.S. Patent No. 4,681,822 (1987).
- ⁹C. M. Berthier and R. H. Friend, U.S. Patent No. 4,734,343 (1988).
- ¹⁰D. F. Shriver and P. G. Bruce, in *Solid State Electrochemistry*, edited by P. G. Bruce (Cambridge University Press, Cambridge, 1995), p. 95.
- ¹¹A. Killis *et al.*, *Solid State Ionics* **14**, 231 (1984).
- ¹²B. Scrosati, in *Solid State Electrochemistry*, edited by P. G. Bruce (Cambridge University Press, Cambridge, 1995), p. 229.
- ¹³Q. B. Pei and Y. Yang, *Synth. Met.* **80**, 131 (1996).
- ¹⁴F. M. Gray, *RSC Materials Monographs* (RSC, Letchworth, 1997).
- ¹⁵Y. Cao *et al.*, *Appl. Phys. Lett.* **68**, 3218 (1996).
- ¹⁶M. A. Ratner, in *Polymer Electrolyte Reviews 1*, edited by J. R. MacCallum and C. A. Vincent (Elsevier Applied Science, London, 1987), p. 173.
- ¹⁷G. Yu *et al.*, *Chem. Phys. Lett.* **259**, 465 (1996).
- ¹⁸H. F. Ivey, *Electroluminescence and Related Effects* (Academic, London, 1963).
- ¹⁹C. Wagner (unpublished).
- ²⁰W. Weppner, in *Solid State Microbatteries*, edited by J. R. Akridge and M. Balkanski (Plenum, London, 1988), p. 381.
- ²¹W. Weppner, in *Solid State Electrochemistry*, edited by P. G. Bruce (Cambridge University Press, Cambridge, 1995), p. 199.
- ²²P. G. Bruce and F. M. Gray, in *Solid State Electrochemistry*, edited by P. G. Bruce (Cambridge University Press, Cambridge, 1995), p. 119.
- ²³D. L. Smith, *J. Appl. Phys.* **81**, 2869 (1997).
- ²⁴F. Cacialli *et al.*, *Appl. Phys. Lett.* **69**, 3794 (1996).
- ²⁵R. N. Marks *et al.*, *J. Phys.: Condens. Matter* **6**, 1379 (1994).
- ²⁶R. S. Berry, S. A. Rice, and J. Ross, *Physical Chemistry* (Wiley, New York, 1980).
- ²⁷R. D. Armstrong and M. Todd, in *Solid State Electrochemistry*,

- edited by P. G. Bruce (Cambridge University Press, Cambridge, 1995), p. 264.
- ²⁸R. H. Fowler and L. Nordheim, Proc. R. Soc. London, Ser. A **119**, 173 (1928).
- ²⁹E. M. Conwell and M. W. Wu, Appl. Phys. Lett. **70**, 1867 (1997).
- ³⁰S. M. Sze, *The Physics of Semiconductor Devices* (Wiley, New York, 1969).
- ³¹J. G. Simmons, J. Appl. Phys. **34**, 1793 (1963).
- ³²P. S. Davids *et al.*, Appl. Phys. Lett. **69**, 2270 (1996).
- ³³D. J. Dick *et al.*, Adv. Mater. **8**, 985 (1996).
- ³⁴J. J. M. Halls *et al.*, Synth. Met. **77**, 277 (1996).
- ³⁵P. J. Hamer *et al.*, Philos. Mag. B **73**, 367 (1996).
- ³⁶A. Killis *et al.*, Macromolecules **17**, 63 (1984).
- ³⁷J. C. deMello, H. F. Wittmann, and R. H. Friend, Adv. Mater. **9**, 230 (1997).
- ³⁸Q. B. Pei *et al.*, J. Am. Chem. Soc. **118**, 3922 (1996).
- ³⁹I. Riess, and D. Cahen, J. Appl. Phys. **82**, 3147 (1997).
- ⁴⁰I. Riess, J. Phys. Chem. Solids **47**, 129 (1986).
- ⁴¹M. Pope and C. E. Swenberg, *Electronic Processes in Organic Crystals* (Clarendon Press, Oxford, 1982).
- ⁴²T. Wilson and C. Shepperd, *Theory and Practice of Scanning Optical Microscopy* (Academic, New York, 1984).